Chemical Geology 377 (2014) 45–55

Contents lists available at ScienceDirect

Chemical Geology

journal homepage: www.elsevier.com/locate/chemgeo

Hafnium isotope evidence for slab melt contributions in the Central Mexican Volcanic Belt and implications for slab melting in hot and cold slab arcs

Yue Cai [a,b,*], Alexandra LaGatta [a,b,1], Steven L. Goldstein [a,b], Charles H. Langmuir [c], Arturo Gómez-Tuena [d], Ana Lillian Martín-del Pozzo [e], Gerardo Carrasco-Núñez [d]

[a] Lamont-Doherty Earth Observatory of Columbia University, 61 Rt. 9W, Palisades, NY 10964, USA
[b] Department of Earth and Environmental Sciences, Columbia University, 61 Rt. 9W, Palisades, NY 10964, USA
[c] Department of Earth and Planetary Sciences, Harvard University, 20 Oxford St., Cambridge, MA 02138 USA
[d] Centro de Geociencias, Universidad Nacional Autónoma de México, Querétaro 76230, Mexico
[e] Departamento de Vulcanología, Instituto de Geofísica, Universidad Nacional Autónoma de México, Ciudad Universitaria, México D.F. 04510, Mexico

ARTICLE INFO

Article history:
Received 9 September 2013
Received in revised form 1 April 2014
Accepted 1 April 2014
Available online 12 April 2014

Editor: K. Mezger

Keywords:
Subduction zones
Mexican Volcanic Belt
Hf and Nd isotopes
Slab melting
High field strength element partitioning
Arc magma petrogenesis

ABSTRACT

This study presents evidence that Quaternary frontal arc calc-alkaline lavas from Central Mexican Volcanic Belt (CMVB) contain contributions from partial melts of the subducting garnet-bearing eclogitic oceanic crust and sediment, based on chemical and Hf–Nd isotope data. The CMVB includes both calc-alkaline lavas with arc-type trace element patterns such as aqueous fluid mobile element enrichments and high field strength element depletions; and "high-Nb" alkaline lavas with trace element patterns similar to ocean island basalts. The two types of lavas are closely related geographically and temporally. Distinct from the high-Nb lavas, the calc-alkaline lavas show trends toward higher $^{176}Hf/^{177}Hf$ and $^{143}Nd/^{144}Nd$ ratios coupled with lower Lu/Hf. The high Hf–Nd isotope ratios fingerprint contributions of subducted basaltic ocean crust, while the correlation with low Lu/Hf indicates melting in the presence of residual garnet, which reflects conversion of the subducted oceanic crust to eclogite. Isotopic and chemical mass balance considerations indicate that the slab melts are ~80% basaltic oceanic crust and ~20% subducted sediment. The calc-alkaline lavas have higher SiO_2 at a given Mg# compared to the high-Nb alkaline lavas, also reflecting melt contributions from the subducted slab.

A survey of global arc lavas shows that calc-alkaline lavas with low Lu/Hf ratios, reflecting melting in the presence of residual garnet and preferential mobilization of Hf over Lu from the subducted slab, are generally associated with hot slab conditions. These include arcs where young (<30 Ma old) ocean crust is subducted (*e.g.* Mexican Volcanic Belt, Cascades, Austral Andes, Luzon, Setouchi), where slab tearing occurred and hot asthenospheric mantle could upwell through the slab window (*e.g.*, western Aleutians, Sunda, southern Scotia), and where oblique or slow subduction leads to higher slab temperatures (*e.g.* Lesser Antilles, western Aleutians). In some of these hot slab arcs, where low Lu/Hf ratios are coupled with high Nd–Hf isotope ratios, slab melt contributions are dominated by partial melts from the subducted oceanic basalt (*e.g.*, Mexican Volcanic Belt, Aleutians and Cascades). In other hot slab arcs, low Lu/Hf ratios are coupled with low Nd–Hf isotope ratios, reflecting slab contributions dominated by sediment melts (*e.g.* Setouchi, Lesser Antilles, Luzon, Sunda, and southern Scotia). Arcs associated with colder subducted oceanic crust (*e.g.* Izu–Bonin–Marianas, Tonga–Kermadec, central and northern Scotia) erupt lavas with high Lu/Hf along with high Hf–Nd isotope ratios, similar to mid-ocean ridge basalts, thus they lack the signature of residual garnet as well as significant slab melt input.

1. Introduction

Magma genesis at convergent plate margins has long been attributed to fluxing of the mantle wedge by "solute-rich" fluids containing significant amounts of H_2O, derived from the subducting oceanic crust and sediments (*e.g.*, Morris et al., 2003; Plank et al., 2009). These fluids also impart distinctive geochemical signatures to arc magmas, such as enrichments in aqueous fluid mobile elements (*e.g.*, Ba, Sr, Pb) relative to elements with limited aqueous fluid mobility, for example the rare

* Corresponding author at: Lamont-Doherty Earth Observatory of Columbia University, 61 Rt. 9W, Palisades, NY 10964, USA.
E-mail address: cai@ldeo.columbia.edu (Y. Cai).
[1] Present address: Department of Environmental Science and Studies, St. Mary's College of California, 1928 St. Mary's Road, Moraga, CA 94556, USA.

http://dx.doi.org/10.1016/j.chemgeo.2014.04.002
0009-2541/

earth elements (REE, *e.g.*, Sm, Nd) and the high field strength elements (HFSE, *e.g.*, Nb, Ta, Hf). It has remained unclear, however, in what capacity silicate melts of the subducted oceanic crust-sediment package contribute to the arc mantle wedge, for example, whether the subducted slab could partially melt under most arcs (*e.g.* Kelemen et al., 2003; Schmidt et al., 2004; Portnyagin et al., 2007); or whether it can only partially melt under unusually hot conditions, such as the subduction of young, hot slabs (*e.g.*, Defant and Drummond, 1990; Peacock et al., 1994), or at slab edges heated by upwelling hot asthenospheric mantle (*e.g.*, Yogodzinski et al., 1995, 2001; Thorkelson and Breitsprecher, 2005). It has also been shown that higher slab temperatures lead to increased silica polymerization and as a result, higher overall trace element mobility (Manning, 2004). Thus, high temperature silica-rich "slab-melts" can be traced by elements with limited mobility in low temperature aqueous- or solute-rich fluids, such as the REE, HFSE and Th. Of particular interest are the heavy rare earth elements (HREE, *e.g.*, Lu, Yb), which are preferentially retained by residual garnet in the slab during eclogite melting.

A challenge in identifying subduction contributions in arc lavas arises from compositional similarities between the subducted package and the overlying mantle-crust assemblage. For example, sediment melt contributions could impose elevated Si content and crustal-like isotope signatures on arc lavas, which resemble the effects of shallow level assimilation-fractional crystallization (AFC) processes (*e.g.*, Hildreth and Moorbath, 1988). Hf–Nd isotopes can be used to identify hydrothermal sediment melt contributions in arcs owing to their distinct Hf–Nd isotope compositions. In Hf–Nd isotope space, most terrestrial rocks (e.g., mafic and felsic volcanics, and clastic sediments) fall on a well-defined "mantle–crust array" (*e.g.* Vervoort et al., 1999, 2011), while hydrothermal sediments fall on a "seawater array", which intersects the "mantle–crust array" at an angle, with higher $^{176}Hf/^{177}Hf$ ratios for a given $^{143}Nd/^{144}Nd$ ratio (Albarède et al., 1998). Melt contributions from subducted hydrothermal sediments could thus generate deviations from the "mantle–crust array" towards the "seawater array" in arc lavas (*e.g.*, Marini et al., 2005; Handley et al., 2011). Moreover slab-derived melt contributions must also be distinguished from melts of the lower crust beneath an arc, which can be evaluated based on relationships between Hf–Nd isotope ratios and high field strength element ratios (*e.g.*, Nb/Ta and Zr/Hf) (*e.g.* Gómez-Tuena et al., 2003; Pfänder et al., 2007; Gómez-Tuena et al., 2011; Pfänder et al., 2012).

Volcanism in the Central Mexican Volcanic Belt (CMVB) is associated with the subduction of the young (14-18 Ma) Cocos Plate (at ~6 cm/year) (Fig. 1; Pardo and Suárez, 1995). The Mexican Volcanic Belt trends oblique to the trench, which reflects an unusual subduction geometry, whereby the subducting Cocos Plate flattens northward and remains at a shallow depth of ~40 km for about 200 km, before it bends down at ~75° angle just below the arc front (Pérez-Campos et al., 2008). Besides subduction of a young, hot oceanic plate, the unusual subduction geometry may also lead to higher slab temperatures given the increased coupling surface between the flat slab and the overlying plate (Manea et al., 2004, 2005). Thus, the CMVB provides an excellent framework to test for slab melting using geochemical tracers.

Evidence for slab melt contributions in the CMVB has been reported in previous studies (*e.g.*, Gómez-Tuena et al., 2003; Martínez-Serrano et al., 2004; Gómez-Tuena et al., 2007; Mori et al., 2007; Gómez-Tuena et al., 2008), although the same types of observations have also been used to argue for crustal assimilation (*e.g.*, Siebe et al., 2004; Schaaf et al., 2005; Torres-Alvarado et al., 2011). However these studies did not report Hf isotope ratios which, as we show here, add important supporting evidence for slab melt contributions. In this study we evaluate the role of slab melting beneath the CMVB with new Hf–Nd isotope and elemental data. To further demonstrate the validity and implications of our findings we also compare our CMVB observations with global arcs.

2. Geologic background

The CMVB is constructed on 45–50 km of continental crust composed of Mesozoic marine sediments overlying Proterozoic granulitic lower crust (Schaaf et al., 1994; Ortega-Gutiérrez et al., 1995;

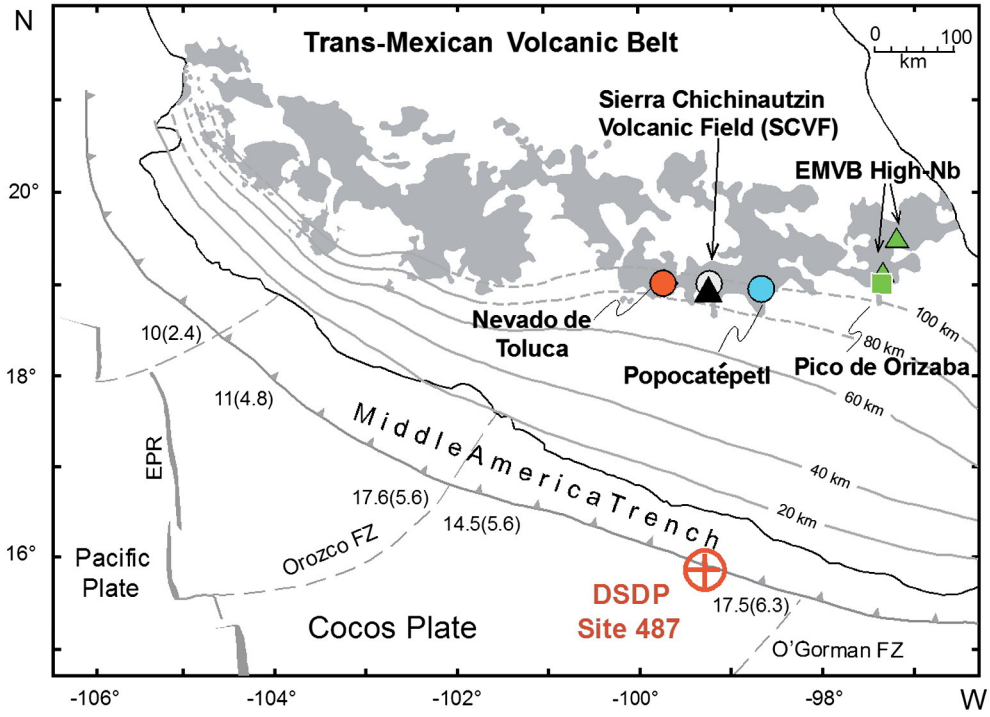

Fig. 1. Schematic map of the studied areas in the context of the Quaternary Trans-Mexican Volcanic Belt (highlighted in dark gray) overlain by contours of inferred slab depth (Pardo and Suárez, 1995). Also shown is the location of DSDP Site 487. "High-Nb" lavas (in triangles) are found in Sierra Chichinautzin Volcanic Field (SCVF) as well as in the Eastern Mexican Volcanic Belt (EMVB) from monogenetic centers near stratovolcano Pico de Orizaba. Other symbols are: EPR = East Pacific Rise; FZ = fracture zone. Along the Middle America Trench, ages of the subducting Cocos plate are marked in millions of years, followed by the convergence rates in parentheses in cm/year (Demets et al., 1990).

Urrutia-Fucugauchi, 1996; Centeno-García et al., 2008; Ortega-Gutiérrez et al., 2008, 2012). Despite passage through the thick continental crust, mafic lavas with high Mg# ($100 * Mg / (Mg + Fe^{2+})$) and Ni contents are common in the CMVB, especially from cinder cones and fissure eruptions (Wallace and Carmichael, 1999; Siebe et al., 2004; Straub et al., 2008, 2011). The unusual occurrence of mafic, near-parental lavas in a thick crust continental arc has been associated with the extensional tectonic stress regime in the region (García-Palomo et al., 2000; Suter et al., 2001). The stratovolcanoes mainly erupt calc-alkaline (CA) lavas, while the mildly alkaline "high-Nb" lavas are only found in some of the monogenetic volcanic centers. The CA lavas show classic arc geochemical signatures, including enrichments in aqueous fluid mobile/immobile elements, and depletions in Nb and Ta (Nb 2–10 ppm, Nb/Th < 3). Many CMVB CA lavas fall into the category of high-Mg# andesites, with 52–63 wt.% SiO_2 and Mg# > 45 (Kelemen et al., 2003; Martínez-Serrano et al., 2004; Gómez-Tuena et al., 2007, 2008). The CMVB CA lavas included in this study are from stratovolcanoes Nevado de Toluca (Toluca), Popocatépetl (Popo), their nearby monogenetic cinder cones, and from Sierra Chichinautzin Volcanic Field (SCVF) (Fig. 1). To evaluate the effects of crustal assimilation, we also compare our CMVB results with lavas from Pico de Orizaba (Orizaba) in the eastern Mexico Volcanic Belt (EMVB), where magma assimilation of Proterozoic lower crustal material has been suggested (e.g., LaGatta, 2003).

High-Nb arc lavas are common in the MVB, despite being volumetrically small and restricted to monogenetic centers (Luhr et al., 2006). They are often found adjacent to CA lavas. The high-Nb lavas we studied are from the SCVF and from cinder cones near EMVB volcano Pico de Orizaba (Fig. 1). The high-Nb lavas show elevated Nb and Ta contents (Nb > 16 ppm, Nb/Th > 6), and minimal enrichment in aqueous fluid mobile elements (*e.g.*, low Ba/Th and U/La) (LaGatta, 2003) (Fig. A1). Both the CA and the high-Nb lavas contain high-Ni olivines, which have been interpreted as evidence for contributions of slab-derived silica-rich liquids (*e.g.* Straub et al., 2008, 2011). However, the high-Nb lavas show lower SiO_2 contents at a given Mg#, and lower $^{87}Sr/^{86}Sr$ at a given $^{143}Nd/^{144}Nd$ ratio, relative to CMVB CA lavas (*e.g.* LaGatta, 2003; Siebe et al., 2004). This is consistent with overall lower slab contributions to the high-Nb lavas (Fig. 2). Based on these characteristics, the high-Nb lavas are generally thought to more closely represent partial melts of the mantle wedge with less slab contributions than the CA lavas (Luhr, 1997; Wallace and Carmichael, 1999; Gómez-Tuena et al., 2003; Siebe et al., 2004).

The sediments and basaltic oceanic crust that are subducting beneath the CMVB are sampled by DSDP Site 487, outboard the trench near Acapulco (Watkins et al., 1981). The sediment column consists of an upper 105 m layer of Quaternary hemipelagic gray mud (called here *terrigenous sediments*) and a lower 65 m layer of Miocene–Pliocene pelagic brown clay with hydrothermal contributions (called here *hydrothermal sediments*) (Watkins et al., 1981). The terrigenous sediments compositionally resemble upper continental crust, while the hydrothermal sediments show elevated Fe and Mn, negative Ce anomalies, and East Pacific Rise mid-ocean ridge basalt-like (EPR MORB) Pb isotope ratios (Verma, 2000; LaGatta, 2003).

3. Analytical methods

Column chromatographic procedures were carried out in the clean chemistry lab at Lamont-Doherty Earth Observatory (LDEO). Volcanic samples were dissolved using a mixture of double-distilled HNO_3 and SeaStar® HF in capped teflon vials. In order to ensure total dissolution of residual minerals, sediment samples were first sintered in a muffle furnace with low blank Na_2O_2 (Fluka®, purum ≥ 95%) (Kleinhanns et al., 2002). Hf was extracted using Eichrom Ln resin (Münker et al., 2001). Nd was extracted using Eichrom TRU® resin followed by BioRad® AG50-X8 resin and alpha-hydroxyisobutyric acid (alpha-HIBA).

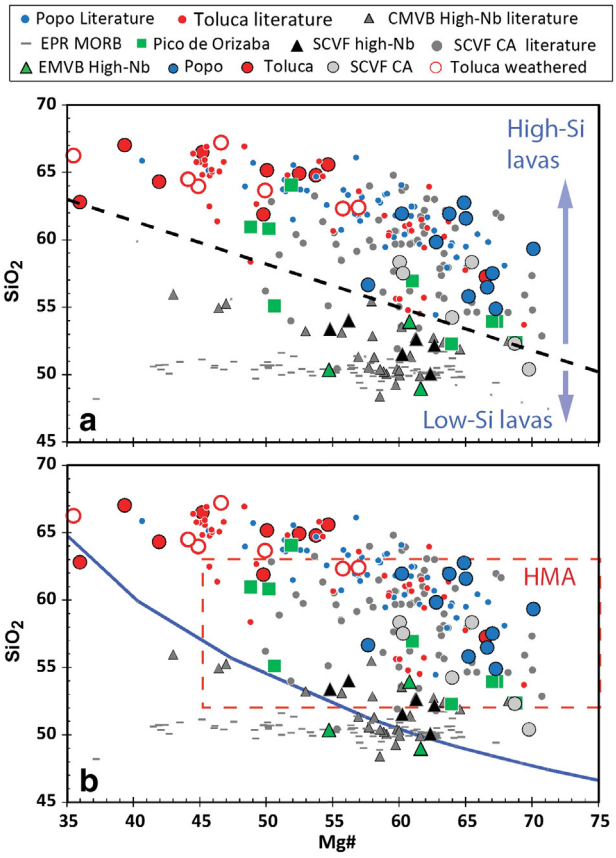

Fig. 2. Mg# *vs.* SiO_2 of studied MVB lavas (large symbols), MVB literature data (small symbols) and MORB data from the northern hemisphere East Pacific Rise (EPR). Panel a shows the SiO_2–Mg# division line that separates CMVB CA lavas from CMVB high-Nb lavas using $SiO_2 = 74.375–0.325 \times Mg\#$. This division line is used later in the discussion of global data in Section 5.5.1, where lavas above the line (*e.g.*, CMVB CA lavas) and below the line (*e.g.*, MVB high-Nb lavas and MORB) are referred to as high- and low-SiO_2 lavas, respectively. The difference between these two groups of lavas cannot be explained by shallow level crustal assimilation, as SiO_2 contents vary greatly at the same Mg#. Instead, addition of slab derived silica-rich liquids is critical for the formation of the high-SiO_2 lavas. Panel b shows the same data in the context of high-Mg# andesites (=HMA) defined by Kelemen et al. (2003) and the tholeiite-calc-alkaline lava division line from Miyashiro (1974). MVB data are from this study, and LaGatta (2003), Schaaf et al. (2005), Martínez-Serrano et al. (2004), Siebe et al. (2004) and Torres-Alvarado et al. (2011). MORB data are from Class and Lehnert (2011).

Hf isotope ratios were measured on a VG-Axiom MC-ICP-MS in the LDEO-AMNH (American Museum of Natural History) ICPMS Lab at LDEO. Nd isotope ratios were measured on a VG-Sector 54 thermal ionization mass spectrometer (TIMS) at LDEO. Additional analytical details are listed in Table EA1. Major elements of the Toluca samples were determined by X-ray fluorescence spectroscopy (XRF) at the Laboratorio Universitario de Geoquímica Isotópica (LUGIS), UNAM, using procedures of Lozano and Bernal (2005). Trace elements were measured by a Thermo Scientific Electron X-series inductively coupled plasma mass spectrometer (ICP-MS) at the Centro de Geociencias (CGEO) at the Universidad Nacional Autónoma de México (UNAM) following sample preparation and measurement procedures described in Mori et al. (2007). The long-term reproducibility of international standard trace element data at CGEO has been reported in several previous publications (*e.g.*, Mori et al., 2007; Gómez-Tuena et al., 2011).

4. Results

We report major element, trace element, Nd and Hf isotope analyses of 13 Toluca lavas (Table EA1); Hf isotope analyses of 5 sediment samples and one basalt sample from DSDP Site 487 (Table EA2); Nd and Hf isotope analyses of 6 piston core sediment samples from the Cocos

plate (Table EA5) obtained from the LDEO Core Repository; and Hf isotope analyses of 38 lavas from the central and eastern MVB (Table EA2), which were selected from a larger sample set based on available elemental and Sr–Pb–Nd isotope data (LaGatta, 2003) to best constrain the effect of shallow level assimilation and slab contributions. Nd isotope ratios are listed as εNd, the deviation in parts per 10,000 from a "chondritic uniform reservoir" (CHUR) value of $^{143}Nd/^{144}Nd$ =0.512638 (Jacobsen and Wasserburg, 1980). Hf isotope ratios are listed as εHf, the deviation in parts per 10,000 from a CHUR value of $^{176}Hf/^{177}Hf$ = 0.282772 (Blichert-Toft and Albarède, 1997). To better compare with older literature data in the diagrams, we did not use the newer CHUR value of 0.282785 (Bouvier et al., 2008), which would decrease all εHf data by ~0.46 εHf units.

For the DSDP Site 487 samples, the terrigenous sediments have the lowest εHf values (−0.7 to +1.0), the basalt has the highest εHf value (+18.1), and the hydrothermal sediments are intermediate (~+6) (Table EA2). In Hf–Nd isotope space (Fig. 3a,b), the terrigenous sediments and the basalt fall on the "mantle–crust array" (Vervoort et al., 1999, 2011), while the hydrothermal sediments overlap with piston core sediments from the Cocos plate further south and they all fall on the "seawater array" (Figs. 3a,b and A6, Albarède et al., 1998).

εHf values in CMVB lavas range from −0.6 to +11.4 (Fig. 3). All measured CMVB lavas fall close to the Hf–Nd mantle–crust array (Vervoort et al., 2011). EMVB Orizaba lavas have the lowest εHf values (−0.6 to 4.2). Hf isotope ratios of CMVB CA lavas (εHf = 4.6 to 11.4) and high-Nb lavas (εHf = 3.4 to 9.1) overlap, but the CA volcanics have the highest εHf–εNd values. In Hf–Nd isotope space, the CA lavas trend from the field of the high-Nb lavas towards a component that resembles EPR MORB, with higher εHf and εNd (Fig. 3a). Our Nd isotope compositions (εNd = 4.4 to 6.3) are comparable with those published by Martínez-Serrano et al. (2004) (εNd = 3.8 to 6.7). Our average Toluca samples show εNd = 5.19 ± 1.18 (2σ, n = 17) which overlaps with earlier results (εNd = 4.94 ± 1.20, n = 21; Martínez-Serrano et al., 2004). D'Antonio (2008) reported two of the same samples (RAM101 and RAM22) with much lower εNd values. Thus, we duplicated the analyses on new splits of the samples in question, and our results are reproducible (Table EA1). The average εNd of Toluca lavas from D'Antonio (2008) is 2.70 ± 2.16 (2σ, n = 8), which differs significantly from the results from our study and Martínez-Serrano et al. (2004). Given these considerations, we stand by our results until further tests are conducted.

Despite our efforts to choose fresh samples, a few samples from Toluca show negative Ce anomalies and elevated REE contents. These characteristics are sometimes associated with incipient weathering (*e.g.*, Price et al., 1991), whereby trivalent REE are mobilized from glassy or fine-grained matrix material, but Ce^{+4} is less mobilized. The weathering effect does not affect the Nd and Hf isotope ratios of our samples (Fig. A2), which suggest that the additional REE are locally derived. Thus, we include these samples in our discussion.

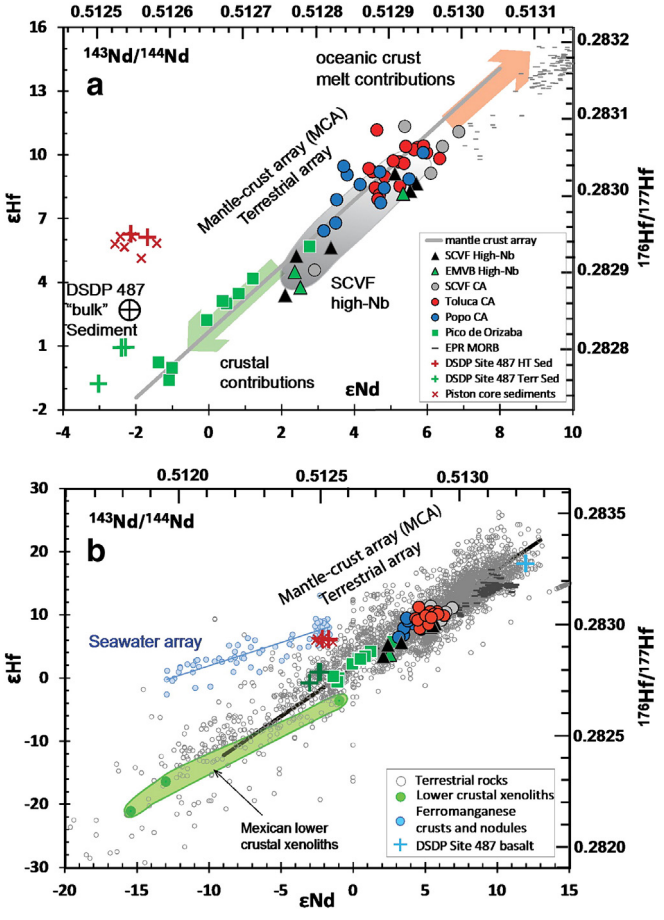

Fig. 3. a) εNd *vs.* εHf of studied MVB lavas; sediments and basalts sampled at DSDP Site 487; and piston core sediments. b) MVB data in the context of the Mexican lower crustal xenoliths (Roberts and Ruiz, 1989; Vervoort et al., 2000); the Nd–Hf mantle–crust array with data from GEOROC, PetDB, Vervoort et al. (1999, 2000, 2011) and Salters et al. (2011); the seawater array based on data from Godfrey et al. (1997), Albarède et al. (1998), David et al. (2001), and van de Flierdt et al. (2004). HT sed = hydrothermal sediments. Terr sed = terrigenous sediments. The DSDP Site 487 "bulk" sediment composition is calculated based on HT: Terr = 4:6 based on the stratigraphy (LaGatta, 2003).

5. Discussion

5.1. Effects of crustal assimilation?

The CMVB lies on thick continental crust and some studies have discussed the potential impact of crustal assimilation to the lavas (*e.g.* Siebe et al., 2004; Schaaf et al., 2005). Magmas that assimilate incompatible element enriched old continental crust would have high $^{87}Sr/^{86}Sr$, $^{207}Pb/^{204}Pb$ ratios, and low εNd and εHf values, coupled with high SiO_2 contents and low Mg#. The Proterozoic lower crust in the CMVB likely has these isotope characteristics, based on low εNd and εHf values observed in lower crustal xenoliths (*e.g.* Patchett and Ruiz, 1987; Schaaf et al., 1994; Vervoort et al., 1999; Ortega-Gutiérrez et al., 2012) and high $^{207}Pb/^{204}Pb$ ratios in granulite outcrop samples (*e.g.* Lawlor et al., 1999). Lavas from Pico de Orizaba, in the EMVB, show evidence of lower crustal assimilation in Pb and Nd isotope space (LaGatta, 2003, Figs. 4, A5). Compared with lavas from Pico de Orizaba in the EMVB, CA lavas from the CMVB show higher εNd–εHf values and their Nd–Pb isotope ratios do not show the "crustal contamination" trend (*e.g.*, Figs. 4, A5; DePaolo, 1981; LaGatta, 2003). Rather they follow well-defined mixing trends in Pb isotope space between a component that is similar to the high-Nb lavas and the terrigenous sediments and a component that is similar to EPR MORB and the hydrothermal sediments (LaGatta, 2003). Olivine phenocrysts that appear to be in equilibrium with CMVB magmas show mantle-like $^{3}He/^{4}He$ ratios (R/Ra > 6.9), which indicates that crustal assimilation is very limited (Straub et al., 2011). Based on these observations, many studies have reached the conclusion that many of the MVB volcanoes erupt surprisingly uncontaminated lavas (*e.g.* Gómez-Tuena et al., 2003; LaGatta, 2003; Martínez-Serrano et al., 2004; Gómez-Tuena et al., 2007; Straub et al., 2008; Schaaf and Carrasco-Núñez, 2010; Straub et al., 2011). These include the volcanoes in this study, and therefore we do not dwell on this issue here. Instead, we will focus on quantifying the slab contributions. We also show (in Section 5.2) that crustal assimilation of an ancient garnet- or amphibole-bearing incompatible element depleted lower crust is unlikely, based on correlations between Hf isotopes and Lu/Hf, Nb/Ta and Zr/Hf ratios.

5.2. Subducted slab contributions to the sub-arc mantle wedge

Sediments are major potential contributors of incompatible elements to the sub-arc mantle (*e.g.* Plank and Langmuir, 1993; Chauvel

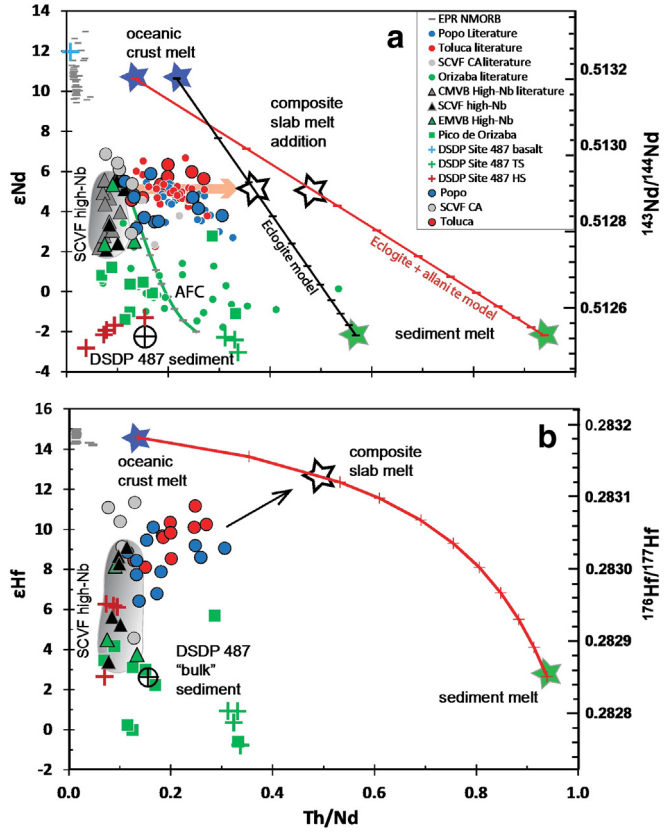

Fig. 4. Th/Nd *vs.* εHf and εNd of MVB lavas and DSDP Site 487 sediments. Only fresh samples with no Ce anomalies are plotted. Also shown are modeled composite slab melt (hollow stars) with two sets of partition coefficients: 1) the black line is an eclogite-only model, where bulk D-values are calculated assuming garnet:cpx = 1 using Kds from Klemme et al. (2002); and 2) the red line is an eclogite + allanite model, which uses bulk D-values from Skora and Blundy (2010). Modeling details are discussed in the text (Section 5.3). The AFC model is calculated using relatively primitive Orizaba lava C46 (Mg# = 67, Table EA2) as the starting composition, and Huiznopala granulite PJL8 (from Lawlor et al., 1999) as the crustal endmember with εNd of −7.45, assuming Ma/Mc = 0.3, D_{Th} = 0.01 and D_{Nd} = 0.1 (DePaolo, 1981). (For interpretation of the references to color in this figure legend, the reader is referred to the web version of this article.)

et al., 2008). Mass balance considerations of sediment subduction along the MVB indicate that most of the sediments reaching the trench are subducted (Watkins et al., 1981). The sediment column sampled by DSDP Site 487 contains a 65 m thick "hydrothermal sediment" unit. Melt contributions containing significant amounts of hydrothermal sediment should generate lavas that trend towards the "seawater array" (Albarède et al., 1998), for example, as seen in the Philippines (Marini et al., 2005). In the CMVB, lavas fall close to the "mantle–crust array", with little indication of Nd–Hf contributions from the subducted hydrothermal sediment (Fig. 3). However, as "bulk" DSDP Site 487 sediment plots close to the mantle crust array, small contributions from sediment melt is hard to discern in Nd–Hf isotope space (Fig. 3b).

High Th/Nd ratios and low εNd values in arc lavas have been used as indicators for contributions of partial melt from the subducted sediments (*e.g.*, Elliott et al., 1997; Plank, 2005). CMVB CA lavas show elevated Th/Nd ratios compared to the high-Nb lavas and EPR MORB (Fig. 4). However, CMVB CA lavas trend toward higher εHf and εNd values with higher Th/Nd ratios, while the DSDP Site 487 sediments have lower εHf and εNd values than the CA lavas. Therefore, the elevated Th/Nd ratios in CMVB CA lavas cannot be simply attributed to the addition of sediment melt, unlike, for example, the Lesser Antilles (Plank, 2005). Instead, contributions from a composite slab melt that is composed of ~80% oceanic crust melt and ~20% sediment melt would generate the observed Th/Nd and Nd–Hf isotope signatures of the CMVB CA lavas (Fig. 4). This scenario is supported by other chemical evidence (shown below), and we demonstrate its validity numerically in Section 5.3.

Considering the depth of the subducting slab under the CMVB, slab melting should occur in the presence of garnet and/or amphibole (Manea et al., 2004). Because HREE strongly partitions into garnet, and to a lesser extent into amphibole (*e.g.* Fulmer et al., 2010 and refs. therein), partial melting of the slab should generate melts with HREE depletions. Fig. 5 shows that for CMVB CA lavas, low Lu/Hf ratios, consistent with a stronger slab melt signature, are associated with higher εHf values. This low Lu/Hf signature is also shown by the steep HREE patterns of the CA lavas (Fig. A1). Hf–Nd isotope ratios of DSDP Site 487 sediment are too low to be the low Lu/Hf, high Th/Nd slab endmember, while the εHf values of EPR MORB are too high (Fig. 5). The slab melt component in the CMVB thus appears to be a composite melt with contributions from both the subducted basalt and ocean sediments.

The question arises regarding whether it is possible to distinguish garnet from amphibole as the residual phase causing the HREE depletion. This question is important because the lower crust could be rich in cumulate amphiboles (Davidson et al., 2007), and although unlikely, they may also have high εNd and εHf values, which could generate the observed correlation of higher εHf with lower Lu/Hf. This question can be addressed using Nb/Ta and Zr/Hf ratios. CMVB CA lavas display large variations in these ratios, and although the correlations are not strong, the lavas with high εNd and εHf values tend to have low Nb/Ta and Zr/Hf ratios (Fig. 6). In order to generate the observed relationships, the high εHf melt source requires $D_{Nb/Ta} > 1$ and $D_{Zr/Hf} > 1$. Amphiboles have $D_{Zr/Hf} \approx 0.6$ (Tiepolo et al., 2007), pyrope-rich garnet typically found in the lower crust also has $D_{Nb/Ta}$ and $D_{Zr/Hf} < 1$ (van Westrenen et al., 1999). Therefore, magma interaction with amphibole and lower-crustal garnet would generate melts with elevated Nb/Ta and Zr/Hf ratios, contrary to our observations. Thus, the most suitable protolith for the melt endmember with high εHf, low Nb/Ta and Zr/Hf ratios appears to be the eclogitic oceanic crust because only grossular-rich garnets have both $D_{Zr/Hf}$ and $D_{Nb/Ta} > 1$ (van Westrenen et al., 1999; Klemme et al., 2002). Rutile, if present in the subducting slab, is likely to dominate the HFSE budget. Experimental studies show that rutile $D_{Nb/Ta}$ depends strongly on melting temperature and/or melt composition (e.g., Linnen and Keppler, 1997). Rutile $D_{Nb/Ta}$ should be > 1 for slab temperatures below 1000 °C with the melt H_2O content below

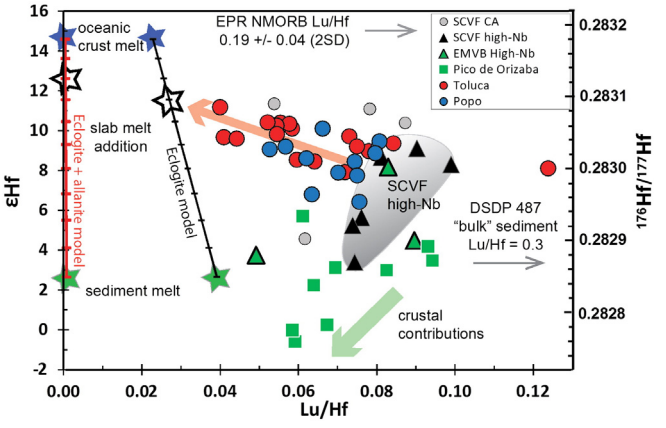

Fig. 5. Lu/Hf *vs.* εHf of MVB lavas, and the modeled composite slab melts (hollow stars). Model parameters are outlined in Fig. 4. The partition coefficients for the HFSE (Nb, Ta, Zr and Hf) are from Skora and Blundy (2010) in both models, as mobility of these elements are largely controlled by rutile in the slab residue. EPR NMORB are samples with $K_2O/TiO_2 < 0.15$ from the compilation of Class and Lehnert (2011). The correlation between Lu/Hf and εHf for the Toluca lavas is statistically significant with r = −0.64 (n = 17), which corresponds to a p-value (probability) < 0.01, or less than a 1% chance that the observed linear correlation could occur at random (Cohen et al., 2003; Soper, 2013). The r-value for CA lavas from both Toluca and Popo is −0.48 (n = 28), which also corresponds to a p-value < 0.01.

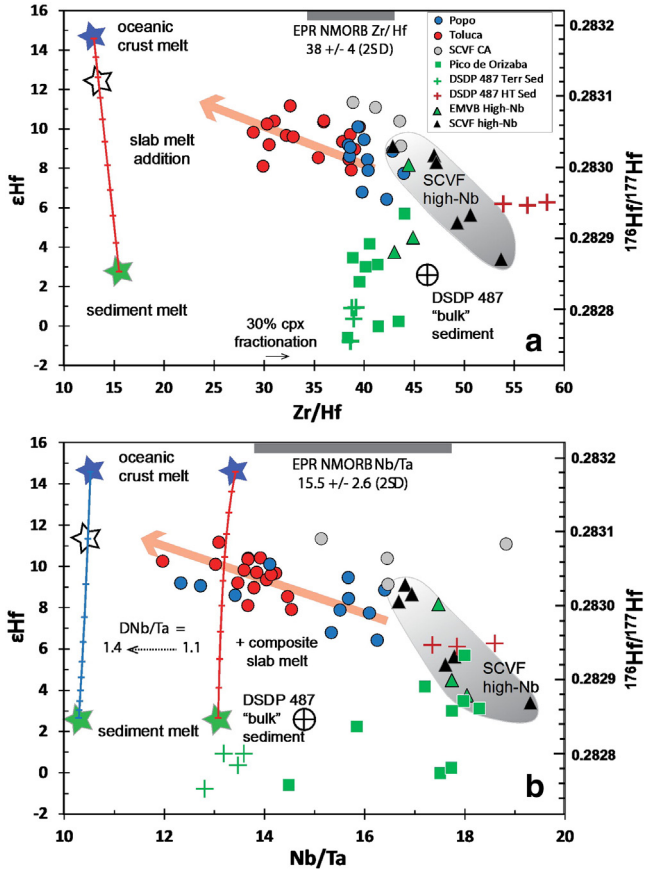

Fig. 6. a) Zr/Hf and b) Nb/Ta *vs.* εHf for MVB lavas and the modeled composite slab melt (hollow stars). The composite slab melt mixing line in red is calculated using $D_{Nb/Ta}$ = 1.1 (Skora and Blundy, 2010), which does not explain the data. However, a higher $D_{Nb/Ta}$ would work (for example $D_{Nb/Ta}$ = 1.4, shown as the blue line). Other model parameters are outlined in Fig. 4.

10 wt.% (Xiong et al., 2011). Slab melting under the CMVB likely occurred under these conditions (Manea et al., 2004). Rutile-bearing eclogite melting experiments at slab P–T conditions also show bulk $D_{Nb/Ta} > 1$ (*e.g.*, Skora and Blundy, 2010). Thus, addition of low degree melts of garnet-bearing eclogitic oceanic crust can account for the higher εHf coupled with the lower Nb/Ta, Zr/Hf and Lu/Hf ratios in CMVB CA lavas, with or without residual rutile.

In summary, the εHf values of EPR MORB are too high to be the only low Lu/Hf–high Th/Nd slab endmember in the CMVB CA lavas (Fig. 5). At the same time, Hf–Nd isotope ratios of DSDP Site 487 sediment are too low to be the endmember. Instead, the low Lu/Hf, Nb/Ta, Zr/Hf and high Th/Nd slab melt component in the CMVB appears to be a composite melt with contributions from the subducted eclogitic oceanic crust and sediments.

EMVB Orizaba lavas, in contrast to the CMVB Toluca, Popo, and SVCF CA lavas, show lower εHf associated with lower Lu/Hf ratios (Fig. 5), which is consistent with assimilation of old lower continental crust containing residual garnet or amphibole. This observation is consistent with Pb isotopic trends from SCVF high-Nb lavas towards Proterozoic age lower crustal granulites (Fig. A5; Lawlor et al., 1999; LaGatta, 2003). However, other observations are not easily explained by lower crustal assimilation. For example, increases in Nb/Ta and Zr/Hf ratios of the magmas would be expected, as both $D_{Zr/Hf}$ and $D_{Nb/Ta}$ would be <1 in a lower crust mineral assemblage that is rich in amphibole and might contain pyrope-rich garnet (van Westrenen et al., 1999; Tiepolo et al., 2007). However, most Orizaba lavas show nearly constant Zr/Hf ratios (Fig. 6). Meanwhile, Nb/Ta ratios of most Orizaba lavas are relatively high and show small variations (Fig. 6), except two samples with low Nb/Ta ratios and εHf values, compatible with some contributions from the subducted sediments. Thus, the HFSE trends in Orizaba lavas are not easily explained by a single process alone, that is, neither lower crustal assimilation (suggested by LaGatta, 2003) nor contributions from subducted sediment (suggested by Schaaf and Carrasco-Núñez, 2010). While both studies would agree that Orizaba lavas contain larger crustal contributions than the CMVB lavas, both crustal assimilation and subduction processes may be contributors.

Finally, the trends of all of the MVB lava series, the CMVB Toluca, Popo and SCVF lavas, as well as the EMVB Orizaba lavas, appear to converge toward a common composition that is similar to the SCVF high-Nb lavas (Figs. 4–6). This common component has higher Lu/Hf than most of the CA lavas and higher εHf–εNd values than the crustally contaminated Orizaba lavas, but lower εHf–εNd values than MORB and the CMVB CA lavas. In agreement with conclusions from previous MVB studies (*e.g.* Luhr, 1997; Wallace and Carmichael, 1999; Gómez-Tuena et al., 2003; Siebe et al., 2004; Schaaf et al., 2005; Blatter et al., 2007), we suggest that Toluca, Popo, Orizaba, and the SCVF lavas share a common, heterogeneous and long-term incompatible element enriched mantle source. We adopt the model proposed by Luhr (1997) for the western MVB, and extended to the CMVB by Wallace and Carmichael (1999), whereby the high-Nb basalts are the first batch of partial melts derived from trench-ward advecting back-arc mantle, and the CA lavas are partial melts derived from the residual mantle after removal of the high-Nb lavas, triggered by further addition of slab derived components.

5.3. Characterizing the slab melt component

The discussion above makes the case for contributions from a composite slab (basaltic ocean crust and sediment) melt to CMVB CA lavas. Here we model the CA lavas by adding slab melts to the CMVB mantle wedge and then partially melt the metasomatized mantle wedge. We constructed a forward model with two main variables: (1) the amount of slab melt addition; (2) the proportion of partial melt from sediment *vs.* basaltic oceanic crust. We solved for these variables to generate the εHf values and Hf contents of CMVB CA lavas (Table EA3).

As we showed above, the high-Nb lavas received less slab contributions than the CA lavas, and they best represent partial melts from a common, long-term incompatible element enriched mantle source, which is most reasonably identified as the upper mantle wedge. The high-Nb lavas have 4–5 times higher Nb and Ta contents than the CA lavas and overall higher REE concentrations, similar to lavas from the back-arc Mexican Basin and Range province (Luhr et al., 2006). This is consistent with the scenario whereby the high-Nb lavas are the first batch of partial melts derived from trench-ward advecting back-arc mantle, and the CA lavas are partial melts derived from the residual mantle after removal of the high-Nb lavas (Luhr, 1997; Wallace and Carmichael, 1999). Based on this model, the mantle wedge under the CMVB could be estimated as the residual mantle (C_s) after extraction of the high-Nb lavas (C_l) using the equation $C_s = C_l \times D$. We used a primitive SCVF high-Nb lava sample, ASC45B, after correction for olivine fractionation, to represent C_l, and the bulk D of spinel lherzolite from Salters and Stracke (2004). The composition of the CMVB mantle wedge can be solved as C_s. The calculated "residual mantle" trace element composition is similar to published "depleted MORB mantle" compositions of Salters and Stracke (2004) and Workman and Hart (2005) (Table EA3, Fig. A7a).

The "bulk" subducting sediment is approximated as the weighted average sediment composition from DSDP Site 487 (LaGatta, 2003). Shallow piston core sediments from the young Cocos plate further to the south and close to the EPR also show typical hydrothermal sediment signatures and overlap with DSDP Site 487 hydrothermal sediments in Nd–Hf isotope space (Figs. 3, A6; Table EA5). Even though more analyses of sediments along the trench are necessary to fully evaluate the subducted sediment component at the CMVB, given the available

evidence, it is reasonable to assume that DSDP Site 487 sediments are representative of the subducting sediments beneath the CMVB. However, the basalts sampled from DSDP Site 487 are restricted to a few altered samples that show unusually depleted incompatible element abundances relative to NMORB (Verma, 2000 and Fig. A1), which is not representative of the oceanic crust. Therefore, we use average "EPR NMORB" from PetDB (Class and Lehnert, 2011) to represent the subducted oceanic crust.

Finding a set of realistic and internally consistent D-values to model the slab melt is a challenge. For example, experiments with eclogite-only protoliths generate $D_{La} \approx 0.02$ (Klemme et al., 2002), which results in grossly over-estimated REE contents (*cf.* model 2, Table EA3). This likely indicates retention of REE by residual allanite and/or monazite in the slab in nature (Klimm et al., 2008). D_{La} from experimental studies with REE doped bulk slab protoliths are much higher but highly variable, from 0.09 to 25.1 (3–4 GPa, 800–900 °C) (Table EA3; Kessel et al., 2005; Klimm et al., 2008; Hermann and Rubatto, 2009). Some of these mobility data are difficult to reconcile with typical arc lava compositions, where LREE are generally enriched. These discrepancies may reflect formation of variable amounts of allanite/monazite in the experiments, which depends on the REE contents of the starting compositions (Klimm et al., 2008). Similar problems exist for D_{HFSE} due to residual rutile and zircon in the experiments. These results also suggest that partition coefficients for these elements may differ greatly between arcs, depending on the composition and metamorphic history of the subducted package under the arc front. We found that D-values from Skora and Blundy (2010) at 900 °C and 3 GPa are more realistic for modeling the slab component with $D_{Nb} = 3.12$, $D_{Ta} = 2.8$, $D_{La} = 0.63$ and $D_{Hf} = 0.5$ (Table EA3).

Our model solves for Hf concentrations as Hf is relatively unaffected by these accessory minerals. Based on the Hf content and εHf value of the lava sample with the strongest slab melt signature (AN182 from Toluca), ~9 wt.% addition of slab melt, composed of oceanic crust melt (F = 1%, F represents degrees of melting) and sediment melt (F = 5%) in a proportion of ~4:1, to the modeled CMVB mantle wedge (plotted in Fig. A7a) could reproduce the key geochemical characteristics observed in CMVB CA lavas, including La and Lu contents; εNd value; lower Nb/Ta, Zr/Hf, Lu/Hf and higher Th/Nd ratios than the high-Nb lavas (Table EA3; Figs. 7b, A7b). The elemental concentrations are more difficult to constrain. However, our results are comparable with typical CMVB CA lavas (Fig. A7b). Based on the model, ~54% of Hf and ~38% of Nd in CMVB CA lavas originate from subducted basalt, and only ~12% of Hf originates from subducted sediment (~5% from the hydrothermal sediment) compared with ~36% of Nd from subducted sediment (Table EA4).

5.4. Summary of the primary observations and implications from Mexico

Despite eruption through thick continental crust, shallow level crustal assimilation does not substantially affect the Nd–Hf isotope and trace element compositions of Quaternary CMVB CA lavas. The CA lavas show typical arc trace element signatures while the high-Nb lavas show oceanic basalt-like signatures for all but a few incompatible elements. The CA lavas show elevated Th/Nd ratios compared to the high-Nb lavas, which are coupled with high Hf–Nd isotope ratios (Fig. 4). We attribute this to contributions of a composite slab melt with ~20% sediment melt and ~80% oceanic crust melt. Our hypothesis is supported by low Lu/Hf ratios of the CA lavas that are coupled with high εHf (and εNd), in contrast to trends delineated by the high-Nb lavas and crustally contaminated EMVB lavas (Fig. 5). The composite slab melt component also has low Nb/Ta and Zr/Hf ratios, consistent with generation by melts equilibrated with grossular-rich garnets found in subducted Ca-rich eclogitic oceanic crust (Fig. 6). Finally, the modeling shows that although hydrothermal sediment melt contributes to the composite slab melt and is added to the mantle wedge source of CMVB lavas, it does not cause a strong offset from the mantle–crust array in Hf–Nd isotope space toward the "seawater array" (Fig. 3). Rather a consequence of the domination of the composite slab melt by basaltic oceanic crust is that the CMVB lavas show only small deviations from the Hf–Nd "mantle crust array" (Fig. 7), even though some of the Hf and Nd are contributed by hydrothermal sediments that plot on the "seawater array".

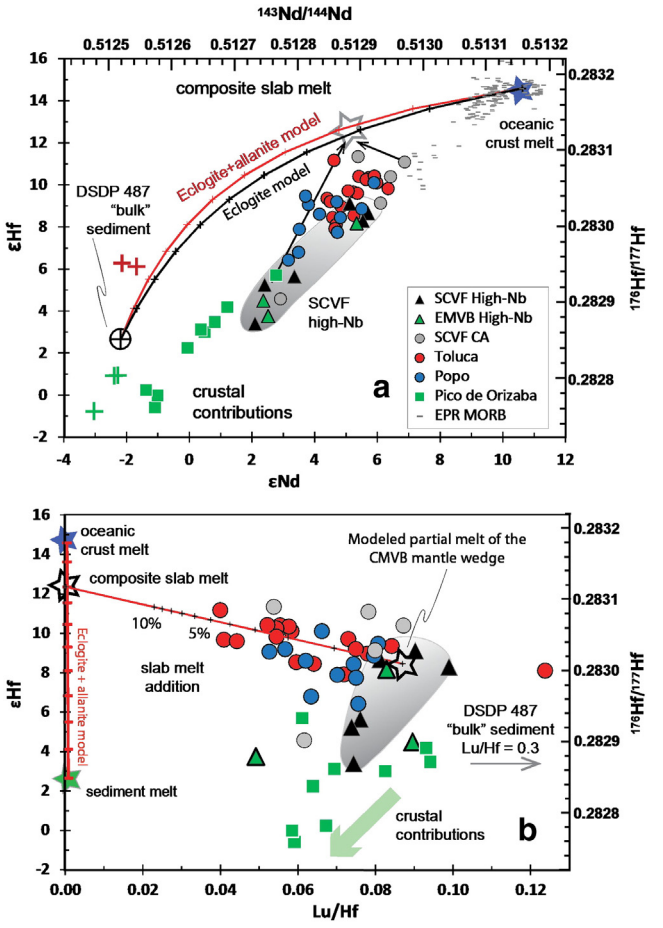

Fig. 7. a) εNd *vs.* εHf of MVB lavas and the modeled composite slab melt (hollow stars). Model parameters are outlined in Fig. 4. CA lava compositions are consistent with addition of the slab melts to the modeled CMVB residual mantle. b) Lu/Hf ratios *vs.* Hf isotopes of studied lavas compared to modeled 10% partial melt of the modeled slab melt metasomatized CMVB mantle wedge (using bulk 2 GPa mantle D-values from Salters and Stracke, 2004) after adding 1% to 10% of composition slab melt (model 1, Table EA3). Tick marks correspond to 1% increments of slab melt addition.

5.5. Subducted slab contributions in global arcs

Defant and Drummond (1990) documented the occurrence of "adakites", with geochemical signatures that could be generated by partial melting of the subducted oceanic crust. These include high MgO at high SiO_2, high Sr, and depletions in HREE due to presence of residual garnet. They attributed these signatures to partial melting of young (<25 Ma), hot subducting oceanic plates. More recent experimental studies have shown that silica-rich eclogitic slab melts have low Mg#, and interaction between slab melts and the mantle wedge is critical in generating arc magmas with elevated Mg# and SiO_2 contents (*e.g.* Sen and Dunn, 1994; Rapp et al., 1999). Our observation, that CMVB CA lavas have high SiO_2 contents at given Mg# (Fig. 2), compared to the high-Nb lavas (and MORB), is consistent with partial melting of a mantle wedge that has received contributions of slab derived silica-rich liquids.

Our data, including the covariations between Hf–Nd isotope ratios and Lu/Hf, Th/Nd, Zr/Hf, Nb/Ta ratios (Figs. 4–6), show strong indications of contributions of a composite slab (basaltic ocean crust and

sediment) melt to the frontal arc lavas in the CMVB. Below we compare our observations with other arcs to determine if there are common relationships with our observations in Mexico that indicate slab melt signatures associated with hot slab conditions.

Currently there are limited Hf isotope data on arcs, and many published datasets with Hf or Nd isotope data do not include Lu, Zr, Ta and Hf contents, all of which pose a challenge for putting together a global compilation. Therefore, we focused on the Aleutian arc (where a comprehensive geochemical dataset is available from Kelemen et al., 2003), plus a few other representative arc segments using precompiled datasets from the GEOROC database (http://georoc.mpch-mainz.gwdg.de; Sarbas, 2008). Despite the limited dataset, we draw some first order observations regarding slab melts in global arcs.

5.5.1. Arcs showing subducted basalt signatures

The Aleutian arc lava data compilation (Kelemen et al., 2003) allows us to make a detailed comparison between Aleutian and CMVB lavas. Using the CMVB Mg#–SiO_2 division line between the CA and high-Nb lavas (Fig. 2), we divided Aleutian lavas into high- and low-SiO_2 groups. Similar to CMVB high-SiO_2 CA lavas, the Aleutians high-SiO_2 lavas consistently show stronger slab melt signatures, with lower Lu/Hf and higher εNd than the low-SiO_2 lavas (Fig. 8a). This compositional dichotomy between high- and low-SiO_2 groups exist in lavas with high, medium, and low Mg#, indicating these characteristics are derived from the mantle rather than through crustal assimilation (Fig. 8a). Furthermore, ~80% of the high-SiO_2 lavas come from western Aleutians (west of 174°W), where the subduction is highly oblique and the orthogonal subduction rate is slow. Thus, the low Lu/Hf ratios of the high-SiO_2 lavas from western Aleutians likely reflect contributions of slab-derived Hf and Nd, carried by silica-rich partial melts.

Arc lavas that show strong chemical signatures indicating melting of the subducted basaltic oceanic crust, that is, with high εHf and εNd coupled with low Lu/Hf ratios like CMVB CA lavas, appear to be associated exclusively with hot slab conditions, caused by either a young age of the subducted crust or the regional tectonics, such as slow subduction (Fig. 8b). These include arcs where young hot slabs are being subducted, such as the CMVB, the Austral Andes (a 12–24 Ma oceanic plate subducting at ~2 cm/year, Stern and Kilian, 1996) and the Cascades (a 2–28 Ma oceanic plate subducting at <2 cm/year, Syracuse et al., 2010); and arcs characterized by slow subduction, such as the western Aleutians (<2 cm/year orthogonal subduction rate, Lee and King, 2010).

5.5.2. Arcs showing subducted sediment melt signatures

Some arcs erupt lavas whose slab melt signatures mainly reflect melting of subducted sediments; these arcs also appear to be associated with hot slab conditions. Their characteristics include low εHf and εNd correlating with elevated Th/Yb and low Lu/Hf ratios (Fig. 9, and Woodhead et al., 2001; Tatsumi and Hanyu, 2003; Marini et al., 2005;

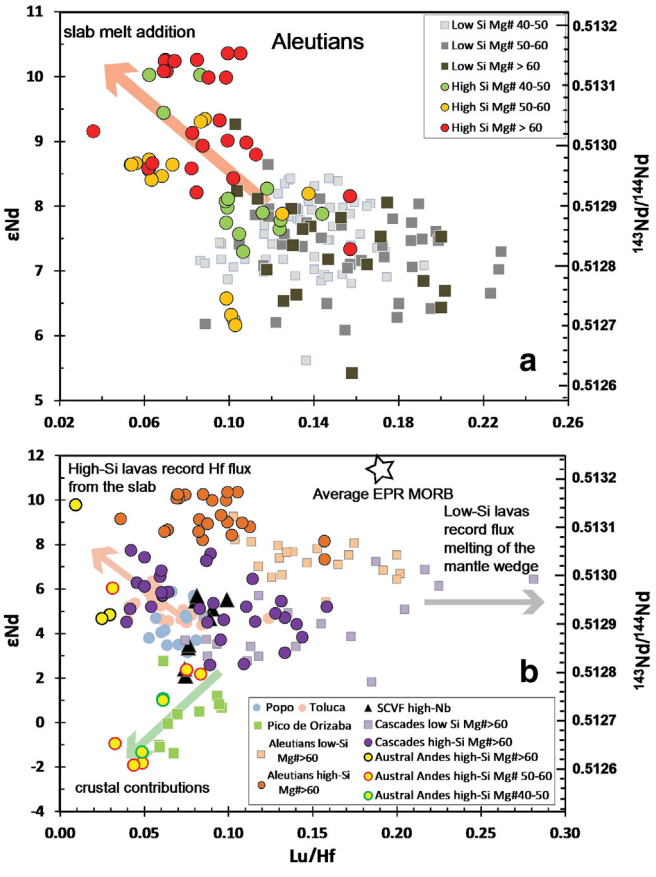

Fig. 8. a) Lu/Hf *vs.* εNd of Aleutian arc lavas divided into high-SiO_2 and low-SiO_2 groups based on the division line in Fig. 2. These compositional groups are further divided based on whole rock Mg#'s to shows that the differences between the two groups are not simply due to shallow level crustal assimilation. The high-SiO_2 group show lower Lu/Hf ratios and higher εNd than the low-SiO_2 group. b) Lu/Hf *vs.* εNd of global arc lavas associated with hot slabs. High-SiO_2 lavas from hot slab arcs generally have lower Lu/Hf ratios and higher εNd than low-SiO_2 lavas, which is consistent with addition of Hf and Nd to the arc mantle through silica-rich liquids from the subducting slabs, with significant contributions from the basaltic crust. Cascades arc data are from GEOROC precompiled datasets (Sarbas, 2008); Austral Andes data from Futa and Stern (1988) and Stern and Kilian (1996); Aleutian data are from Kelemen et al. (2003).

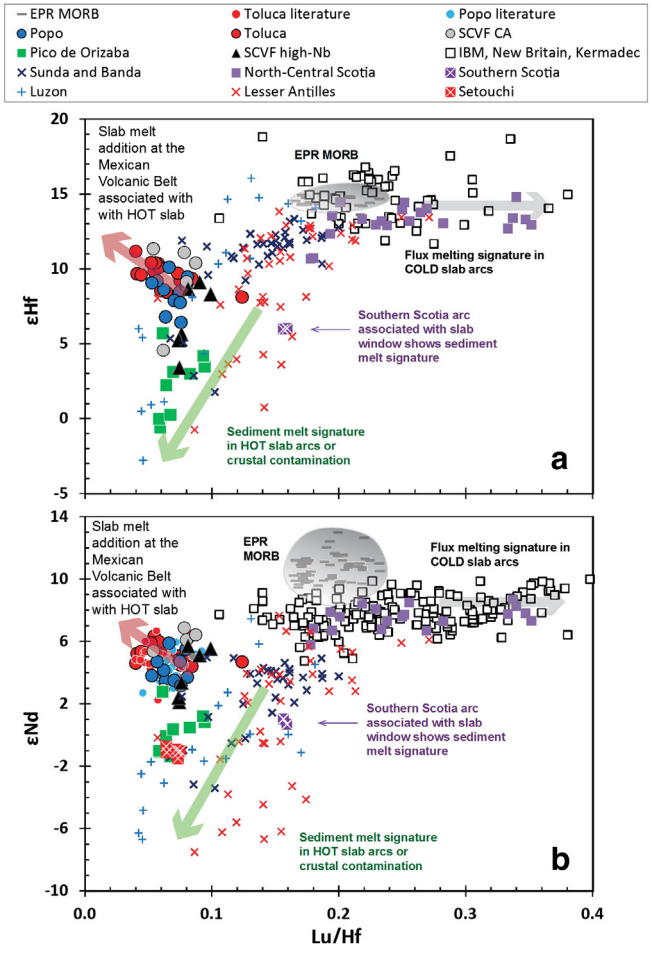

Fig. 9. Lu/Hf *vs.* a) εHf and b) εNd for global arcs. Data sources are: Sunda and Kermadec — Woodhead et al. (2001); Lesser Antilles — Woodhead et al. (2001), Labanieh et al. (2012); Setouchi — Tatsumi and Hanyu (2003); North and Central Scotia (N–C Scotia) and Southern Scotia (S. Scotia) — Barry et al. (2006); Luzon — Marini et al. (2005); Izu–Bonin–Marianas (IBM) data — arc lavas with Mg# = 40–80 are from the GEOROC database (Sarbas, 2008), as well as Woodhead et al. (2001) and Elliott et al. (1997). Tonga data include lavas from frontal arc volcanoes south of 16°S from GEOROC (Sarbas, 2008).

Barry et al., 2006). They also show elevated SiO_2 at high Mg#, akin to high-Mg# andesites (Kelemen et al., 2003). Some of these arcs are clearly associated with young hot subducting slabs, for example, Setouchi which is associated with subduction of ~15 Ma oceanic crust of the Shikoku basin (Tatsumi and Hanyu, 2003 and refs. therein), Luzon which is associated with subduction of ~16–30 Ma South China Sea oceanic crust (Queano et al., 2007 and refs. therein), and a subset of arc lavas from the Austral Andes (Futa and Stern, 1988; Stern and Kilian, 1996). Other arcs in this group that are associated with older subducting slabs may also have elevated slab temperatures due to slow subduction, such as the Lesser Antilles, where ~85 Ma oceanic crust subducts at <1.8 cm/year (Syracuse et al., 2010). Or sediment melting may be associated with slab tearing, which allows hot asthenospheric mantle to upwell through the slab window and heat up the surrounding slab, as in the case of Luzon (Yang et al., 1996), Sunda (Whittaker et al., 2007) and southern Scotia (Barry et al., 2006).

5.5.3. Arcs showing little or no slab melt signatures

Arc lavas that are associated with old and cold subducted oceanic crust appear to erupt lavas with chemical characteristics that mainly reflecting fluid fluxed melting of the mantle wedge, with limited contributions from silicate slab melts. Such characteristics include strong signatures of aqueous fluid mobile elements (*e.g.*, high Ba/La and Sr/Nd ratios, Woodhead et al., 2001), along with high εHf, εNd and high Lu/Hf ratios (Fig. 9). These signatures reflect limited transfer of the HFSE and HREE from the subducting slab to the mantle wedge, and they lack a strong residual garnet signature. These arcs include western Pacific arcs such as the Izu–Bonin–Marianas (with 135–150 Ma old oceanic crust subducting at 1.3–4 cm/year), Tonga–Kermadec (with > 100 Ma old oceanic crust subducting at 5–13 cm/year), as well as the northern and central Scotia arc (with ~59 Ma old oceanic crust subducting at ~5 cm/year) in the Atlantic. The ages and descent rates of the oceanic plates are from Syracuse et al. (2010). Tonga–Kermadec arc is generally considered a cold slab arc (*e.g.*, Plank et al., 2009; Cooper et al., 2012). However, Cooper et al. (2012) consider the Marianas as a hot slab arc, despite the old (~150 Ma) ocean crust. Signatures of sediment melt and slab derived Hf are observed in some Marianas lavas (Elliott et al., 1997; Tollstrup et al., 2010). However, Marianas arc lavas generally show less slab melt contributions than arcs associated with hotter slab conditions.

5.5.4. Global arcs summary

In summary, our global arc compilation suggests that arc chemical signatures indicating melting of subducted oceanic crust or melting of subducted sediment are both associated with hot conditions in the subducted slab. These conditions occur where young oceanic crust is subducted, where older crust is heated during slow subduction, and when the slab is heated by upwelling hot asthenospheric mantle. While the processes that control the proportion of sediment melt *vs.* eclogitic basaltic oceanic crust melt remain unclear, high slab temperatures appear to be required for both scenarios. Other factors that determine whether sediment melt or oceanic crust melt contributions dominate at a given hot slab arc segment may be sediment composition and availability, and slab geometry.

6. Conclusions

Despite erupting through the thick, 45–50 km overlying continental crust, CMVB lavas largely preserve their mantle-derived Nd–Hf isotope and trace element geochemical signatures. Calc-alkaline lavas from the frontal arc show higher Hf isotope ratios correlating with higher Th/Nd ratios and lower Lu/Hf ratios, which fingerprint contributions of a silicate melt derived from the subducting eclogitic oceanic crust and sediments to the arc mantle wedge. This slab melt component also appears to have low Nb/Ta and Zr/Hf ratios, which indicates partial melting of the garnet-bearing eclogitic slab and precludes shallow level crustal assimilation.

Modeling results suggest that partial melting of the CMVB mantle wedge, metasomatized by less than 10% slab derived melt, can explain observed lava Hf–Nd isotope compositions, and the contents and ratios of such trace elements as the HFSE, Th, and the REE, which are not easily mobilized by aqueous fluids and thus are transported by high temperature silicate melts or silica-rich fluids. In the CMVB the composite subducted slab melt is dominated by partial melts from the eclogitic subducted oceanic crust (~80%) relative to subducted sediment (~20%). A consequence of the domination of the composite melt by basaltic oceanic crust is that the CMVB lavas show only small deviations from the Hf–Nd "mantle crust array", even though some of the Hf and Nd are contributed by hydrothermal sediments that plot on the "seawater array" at higher εHf for a given εNd.

An evaluation of global arc lavas shows that the slab silicate melt signatures are absent in western Pacific arcs associated with colder slabs, such as Izu–Bonin–Marianas, Tonga–Kermadec, as well as the northern and central Scotia arc in the Atlantic. Slab melt signatures are mostly found in arcs with hotter slabs, associated with the subduction of young (<30 Ma) oceanic crust, slow subduction, or slab tearing. In some of these arc segments, sediment melt signatures dominate lava chemistry, where low εHf and εNd correlate with low Lu/Hf and elevated Th/Yb ratios (*e.g.*, Luzon in the Philippines, Setouchi in southern Japan, the Lesser Antilles, the southern Scotia arc). Slab melts dominated by subducted basaltic ocean crust are only found in a few arc segments associated with hot slab conditions (*e.g.*, CMVB, Cascades, western Aleutians, and the Austral Andes).

Acknowledgments

We thank Lucia Capra and Gianluca Groppelli for samples from Nevado de Toluca, Ofelia Pérez-Arvizu for performing the trace element analyses at UNAM, Alex Piotrowski and Tina van der Flierdt for assistance in setting up Hf column chemistry, Louise Bolge for help with the ICPMS analyses at LDEO, Susanne Straub for helpful discussions of the CMVB, Terry Plank and David Walker for helpful discussions on geochemical modeling and Peter Kelemen for sharing his precompiled lava dataset of the Aleutians. Some samples in this study were provided by the Lamont-Doherty Core Repository. This study was partly supported by the Storke Endowment of the Department of Earth and Environmental Sciences, Columbia University, and NSF grant (EAR 96-14782) to CHL and SLG. We are grateful to the editor and two anonymous reviewers for their detailed and constructive comments which greatly improved the manuscript. This is LDEO contribution no. 7775.

Appendix A. Supplementary data

Supplementary data to this article can be found online at http://dx.doi.org/10.1016/j.chemgeo.2014.04.002.

References

Albarède, F., Simonetti, A., Vervoort, J.D., Blichert-Toft, J., Abouchami, W., 1998. A Hf–Nd isotopic correlation in ferromanganese nodules. Geophys. Res. Lett. 25, 3895–3898.
Barry, T.L., Pearce, J.A., Leat, P.T., Millar, I.L., le Roex, A.P., 2006. Hf isotope evidence for selective mobility of high-field-strength elements in a subduction setting: South Sandwich Islands. Earth Planet. Sci. Lett. 252, 223–244.
Blatter, D.L., Farmer, G.L., Carmichael, I.S.E., 2007. A north–south transect across the central Mexican volcanic belt at similar to 100 degrees W: spatial distribution, petrological, geochemical, and isotopic characteristics of quaternary volcanism. J. Petrol. 48, 901–950.
Blichert-Toft, J., Albarède, F., 1997. The Lu–Hf isotope geochemistry of chondrites and the evolution of the mantle–crust system. Earth Planet. Sci. Lett. 148, 243–258.
Bouvier, A., Vervoort, J.D., Patchett, P.J., 2008. The Lu–Hf and Sm–Nd isotopic composition of CHUR: constraints from unequilibrated chondrites and implications for the bulk composition of terrestrial planets. Earth Planet. Sci. Lett. 273, 48–57.
Centeno-García, E., Guerrero-Suastegui, M., Talavera-Mendoza, O., 2008. The Guerrero Composite Terrane of western Mexico: collision and subsequent rifting in a supra-

subduction zone. In: Draut, A.E., Clift, P.D., Scholl, D.W. (Eds.), Formation and Applications of the Sedimentary Record in Arc Collision Zones, pp. 279–308.
Chauvel, C., Lewin, E., Carpentier, M., Arndt, N.T., Marini, J.-C., 2008. Role of recycled oceanic basalt and sediment in generating the Hf–Nd mantle array. Nat. Geosci. 1, 64–67.
Class, C., Lehnert, K., 2011. PetDB expert MORB, mid-ocean ridge basalt. Compilation. http://dx.doi.org/10.1594/IEDA/100060.
Cohen, J., Cohen, P., West, S.G., Aiken, L.S., 2003. Applied Multiple Regression/Correlation Analysis for the Behavioral Sciences, 3rd ed. Lawrence Earlbaum Associates, NJ.
Cooper, L.B., Ruscitto, D.M., Plank, T., Wallace, P.J., Syracuse, E.M., Manning, C.E., 2012. Global variations in H_2O/Ce: 1. Slab surface temperatures beneath volcanic arcs. Geochem. Geophys. Geosyst. 13.
D'Antonio, M., 2008. Reconstrucción de los eventos eruptivos de hace ~28 y ~13 ka asociados al emplazamiento de flujos de bloques y ceniza en el volcán Nevado de Toluca (México). UNAM.
David, K., Frank, M., O'Nions, R.K., Belshaw, N.S., Arden, J.W., 2001. The Hf isotope composition of global seawater and the evolution of Hf isotopes in the deep Pacific Ocean from Fe–Mn crusts. Chem. Geol. 178, 23–42.
Davidson, J., Turner, S., Handley, H., Macpherson, C., Dosseto, A., 2007. Amphibole "sponge" in arc crust? Geology 35, 787–790.
Defant, M.J., Drummond, M.S., 1990. Derivation of some modern arc magmas by melting of young subducted lithosphere. Nature 347, 662–665.
Demets, C., Gordon, R.G., Argus, D.F., Stein, S., 1990. Current plate motions. Geophys. J. Int. 101, 425–478.
DePaolo, D.J., 1981. Trace element and isotopic effects of combined wallrock assimilation and fractional crystallization. Earth Planet. Sci. Lett. 53, 189–202.
Elliott, T., Plank, T., Zindler, A., White, W., Bourdon, B., 1997. Element transport from slab to volcanic front at the Mariana arc. J. Geophys. Res. Solid Earth 102, 14991–15019.
Fulmer, E.C., Nebel, O., van Westrenen, W., 2010. High-precision high field strength element partitioning between garnet, amphibole and alkaline melt from Kakanui, New Zealand. Geochim. Cosmochim. Acta 74, 2741–2759.
Futa, K., Stern, C.R., 1988. Sr and Nd isotopic and trace element compositions of Quaternary volcanic centers of the Southern Andes. Earth Planet. Sci. Lett. 88, 253–262.
García-Palomo, A., Macias, J.L., Garduno, V.H., 2000. Miocene to Recent structural evolution of the Nevado de Toluca volcano region, Central Mexico. Tectonophysics 318, 281–302.
Godfrey, L.V., Lee, D.C., Sangrey, W.F., Halliday, A.N., Salters, V.J.M., Hein, J.R., White, W.M., 1997. The Hf isotopic composition of ferromanganese nodules and crusts and hydrothermal manganese deposits: implications for seawater Hf. Earth Planet. Sci. Lett. 151, 91–105.
Gómez-Tuena, A., LaGatta, A.B, Langmuir, C.H., Goldstein, S.L., Ortega-Gutierrez, F., Carrasco-Núñez, G., 2003. Temporal control of subduction magmatism in the eastern Trans-Mexican Volcanic Belt: mantle sources, slab contributions, and crustal contamination. Geochem. Geophys. Geosyst. 4.
Gómez-Tuena, A., Langmuir, C.H., Goldstein, S.L., Straub, S.M., Ortega-Gutierrez, F., 2007. Geochemical evidence for slab melting in the Trans-Mexican Volcanic Belt. J. Petrol. 48, 537–562.
Gómez-Tuena, A., Mori, L., Rincon-Herrera, N.E., Ortega-Gutierrez, F., Sole, J., Iriondo, A., 2008. The origin of a primitive trondhjemite from the Trans-Mexican Volcanic Belt and its implications for the construction of a modern continental arc. Geology 36, 471–474.
Gómez-Tuena, A., Mori, L., Goldstein, S.L., Pérez-Arvizu, O., 2011. Magmatic diversity of western Mexico as a function of metamorphic transformations in the subducted oceanic plate. Geochim. Cosmochim. Acta 75, 213–241.
Handley, H.K., Turner, S., Macpherson, C.G., Gertisser, R., Davidson, J.P., 2011. Hf–Nd isotope and trace element constraints on subduction inputs at island arcs: limitations of Hf anomalies as sediment input indicators. Earth Planet. Sci. Lett. 304, 212–223.
Hermann, J., Rubatto, D., 2009. Accessory phase control on the trace element signature of sediment melts in subduction zones. Chem. Geol. 265, 512–526.
Hildreth, W., Moorbath, S., 1988. Crustal contributions to arc magmatism in the Andes of Central Chile. Contrib. Mineral. Petrol. 98, 455–489.
Jacobsen, S.B., Wasserburg, G.J., 1980. Sm–Nd isotopic evolution of chondrites. Earth Planet. Sci. Lett. 50, 139–155.
Kelemen, P.B., Yogodzinski, G.M., Scholl, D.W., 2003. Along-strike variation in lavas of the Aleutian island arc: implications for the genesis of high Mg# andesite and the continental crust. AGU Monogr. 138.
Kessel, R., Schmidt, M.W., Ulmer, P., Pettke, T., 2005. Trace element signature of subduction-zone fluids, melts and supercritical liquids at 120–180 km depth. Nature 437, 724–727.
Kleinhanns, I.C., Kreissig, K., Kamber, B.S., Meisel, T., Nagler, T.F., Kramers, J.D., 2002. Combined chemical separation of Lu, Hf, Sm, Nd, and REEs from a single rock digest: precise and accurate isotope determinations of Lu–Hf and Sm–Nd using multicollector-ICPMS. Anal. Chem. 74, 67–73.
Klemme, S., Blundy, J.D., Wood, B.J., 2002. Experimental constraints on major and trace element partitioning during partial melting of eclogite. Geochim. Cosmochim. Acta 66, 3109–3123.
Klimm, K., Blundy, J.D., Green, T.H., 2008. Trace element partitioning and accessory phase saturation during H_2O-saturated melting of basalt with implications for subduction zone chemical fluxes. J. Petrol. 49, 523–553.
Labanieh, S., Chauvel, C., Germa, A., Quidelleur, X., 2012. Martinique: a clear case for sediment melting and slab dehydration as a function of distance to the trench. J. Petrol. 53, 2441–2464.
LaGatta, A.B, 2003. Arc Magma Genesis in the Eastern Mexican Volcanic Belt. Columbia University.
Lawlor, P.J., Ortega-Gutierrez, F., Cameron, K.L., Ochoa-Camarillo, H., Lopez, R., Sampson, D.E., 1999. U–Pb geochronology, geochemistry, and provenance of the Grenvillian Huiznopala Gneiss of Eastern Mexico. Precambrian Res. 94, 73–99.
Lee, C., King, S.D., 2010. Why are high-Mg# andesites widespread in the western Aleutians? A numerical model approach. Geology 38, 583–586.
Linnen, R.L., Keppler, H., 1997. Columbite solubility in granitic melts: consequences for the enrichment and fractionation of Nb and Ta in the Earth's crust. Contrib. Mineral. Petrol. 128, 213–227.
Lozano, R., Bernal, J.P., 2005. Characterization of a new set of eight geochemical reference materials for XRF major and trace element analysis. Rev. Mex. Cienc. Geol. 22, 329–344.
Luhr, J.F., 1997. Extensional tectonics and the diverse primitive volcanic rocks in the western Mexican Volcanic Belt. Can. Mineral. 35, 473–500.
Luhr, J.F., Kimberly, P., Siebert, L., Aranda-Gómez, J.J., Housh, T.B., Kysar Mattietti, G., 2006. México's Quaternary volcanic rocks: insights from the MEXPET petrological and geochemical database. Geol. Soc. Am. Spec. Pap. 402, 1–44.
Manea, V.C., Manea, M., Kostoglodov, V., Currie, C.A., Sewell, G., 2004. Thermal structure, coupling and metamorphism in the Mexican subduction zone beneath Guerrero. Geophys. J. Int. 158, 775–784.
Manea, V.C., Manea, M., Kostoglodov, V., Sewell, G., 2005. Thermo-mechanical model of the mantle wedge in Central Mexican subduction zone and a blob tracing approach for the magma transport. Phys. Earth Planet. Inter. 149, 165–186.
Manning, C.E., 2004. The chemistry of subduction-zone fluids. Earth Planet. Sci. Lett. 223, 1–16.
Marini, J.C., Chauvel, C., Maury, R.C., 2005. Hf isotope compositions of northern Luzon arc lavas suggest involvement of pelagic sediments in their source. Contrib. Mineral. Petrol. 149, 216–232.
Martínez-Serrano, R.G., Schaaf, P., Solis-Pichardo, G., Hernandez-Bernal, M.D., Hernandez-Trevino, T., Morales-Contreras, J.J., Macias, J.L., 2004. Sr, Nd and Pb isotope and geochemical data from the Quaternary Nevado de Toluca volcano, a source of recent adakitic magmatism, and the Tenango Volcanic Field, Mexico. J. Volcanol. Geotherm. Res. 138, 77–110.
McDonough, W.F., Sun, S.S., 1995. The composition of the Earth. Chem. Geol. 120, 223–253.
Miyashiro, A., 1974. Volcanic rock series in island arcs and active continental margins. Am. J. Sci. 274, 321–355.
Mori, L., Gómez-Tuena, A., Cai, Y., Goldstein, S.L., 2007. Effects of prolonged flat subduction on the Miocene magmatic record of the central Trans-Mexican Volcanic Belt. Chem. Geol. 244, 452–473.
Morris, J.D., Ryan, J.G., Heinrich, D.H., Karl, K.T., 2003. Subduction Zone Processes and Implications for Changing Composition of the Upper and Lower Mantle, Treatise on Geochemistry. Pergamon, Oxford pp. 451–470.
Münker, C., Weyer, S., Scherer, E., Mezger, K., 2001. Separation of high field strength elements, Nb, Ta, Zr, Hf. and Lu from rock samples for MC-ICPMS measurements. Geochem. Geophys. Geosyst. 2.
Ortega-Gutiérrez, F., Ruiz, J., Centeno-García, E., 1995. Oaxaquia, a Proterozoic microcontinent accreted to North America during the late Paleozoic. Geology 23, 1127–1130.
Ortega-Gutiérrez, F., Elias-Herrera, M., Davalos-Elizondo, M.G., 2008. On the nature and role of the lower crust in the volcanic front of the Trans-Mexican Volcanic Belt and its fore-arc region, southern and central Mexico. Rev. Mex. Cienc. Geol. 25, 346–364.
Ortega-Gutiérrez, F., Elías-Herrera, M., Gómez-Tuena, A., Mori, L., Reyes-Salas, M., Macías-Romo, C., Solari, L.A., 2012. Petrology of high-grade crustal xenoliths in the Chalcatzingo Miocene subvolcanic field, southern Mexico: buried basement of the Guerrero–Morelos platform and tectonostratigraphic implications. Int. Geol. Rev. 54, 1597–1634.
Pardo, M., Suárez, G., 1995. Shape of the subducted Rivera and Cocos Plates in Southern Mexico — seismic anti tectonic implications. J. Geophys. Res. Solid Earth 100, 12357–12373.
Patchett, P.J., Ruiz, J., 1987. Nd isotopic ages of crust formation and metamorphism in the Precambrian of eastern and southern Mexico. Contrib. Mineral. Petrol. 96, 523–528.
Peacock, S.M., Rushmer, T., Thompson, A.B., 1994. Partial melting of subducting oceanic-crust. Earth Planet. Sci. Lett. 121, 227–244.
Pérez-Campos, X., Kim, Y., Husker, A., Davis, P.M., Clayton, R.W., Iglesias, A., Pacheco, J.F., Singh, S.K., Manea, V.C., Gurnis, M., 2008. Horizontal subduction and truncation of the Cocos Plate beneath central Mexico. Geophys. Res. Lett. 35.
Pfänder, J.A., Münker, C., Stracke, A., Mezger, K., 2007. Nb/Ta and Zr/Hf in ocean island basalts — implications for crust–mantle differentiation and the fate of Niobium. Earth Planet. Sci. Lett. 254, 158–172.
Pfänder, J.A., Jung, S., Münker, C., Stracke, A., Mezger, K., 2012. A possible high Nb/Ta reservoir in the continental lithospheric mantle and consequences on the global Nb budget — evidence from continental basalts from Central Germany. Geochim. Cosmochim. Acta 77, 232–251.
Plank, T., 2005. Constraints from thorium/lanthanum on sediment recycling at subduction zones and the evolution of the continents. J. Petrol. 46, 921–944.
Plank, T., Langmuir, C.H., 1993. Tracing trace-elements from sediment input to volcanic output at subduction zones. Nature 362, 739–743.
Plank, T., Cooper, L.B., Manning, C.E., 2009. Emerging geothermometers for estimating slab surface temperatures. Nat. Geosci. 2, 611–615.
Portnyagin, M., Hoernle, K., Plechov, P., Mironov, N., Khubunaya, S., 2007. Constraints on mantle melting and composition and nature of slab components in volcanic arcs from volatiles (H_2O, S, Cl, F) and trace elements in melt inclusions from the Kamchatka Arc. Earth Planet. Sci. Lett. 255, 53–69.
Price, R.C., Gray, C.M., Wilson, R.E., Frey, F.A., Taylor, S.R., 1991. The effects of weathering on rare-earth element, Y and Ba abundances in tertiary basalts from Southeastern Australia. Chem. Geol. 93, 245–265.
Queano, K.L., Ali, J.R., Milsom, J., Aitchison, J.C., Pubellier, M., 2007. North Luzon and the Philippine Sea Plate motion model: insights following paleomagnetic, structural, and age-dating investigations. J. Geophys. Res. Solid Earth 112, B05101.

Rapp, R.P., Shimizu, N., Norman, M.D., Applegate, G.S., 1999. Reaction between slab-derived melts and peridotite in the mantle wedge: experimental constraints at 3.8 GPa. Chem. Geol. 160, 335–356.
Roberts, S.J., Ruiz, J., 1989. Geochemistry of exposed granulite facies terrains and lower crustal xenoliths in Mexico. J. Geophys. Res. Solid Earth Planets 94, 7961–7974.
Ryan, W.B.F., Carbotte, S.M., Coplan, J.O., O'Hara, S., Melkonian, A., Arko, R., Weissel, R.A., Ferrini, V., Goodwillie, A., Nitsche, F., Bonczkowski, J., Zemsky, R., 2009. Global Multi-Resolution Topography synthesis. Geochem. Geophys. Geosyst. 10, Q03014. http://dx.doi.org/10.1029/2008GC002332.
Salters, V.J.M., Stracke, A., 2004. Composition of the depleted mantle. Geochem. Geophys. Geosyst. 5.
Salters, V.J.M., Mallick, S., Hart, S.R., Langmuir, C.E., Stracke, A., 2011. Domains of depleted mantle: new evidence from hafnium and neodymium isotopes. Geochem. Geophys. Geosyst. 12.
Sarbas, B., 2008. The GEOROC database as part of a growing geoinformatics network. In: Brady, S.R., Sinha, A.K., Gundersen, L.C. (Eds.), Geoinformatics 2008—Data to Knowledge, Proceedings: U.S. Geological Survey Scientific Investigations Report 2008-5172. USGS, pp. 42–43.
Schaaf, P., Carrasco-Núñez, G., 2010. Geochemical and isotopic profile of Pico de Orizaba, Citlaltepetl. volcano, Mexico: insights for magma generation processes. J. Volcanol. Geotherm. Res. 197, 108–122.
Schaaf, P., Heinrich, W., Besch, T., 1994. Composition and Sm–Nd isotopic data of the lower crust beneath San-Luis-Potosi, Central Mexico — evidence from a granulite-facies xenolith suite. Chem. Geol. 118, 63–84.
Schaaf, P., Stimac, J., Siebe, C., Macias, J.L., 2005. Geochemical evidence for mantle origin and crustal processes in volcanic rocks from Popocatepetl and surrounding monogenetic volcanoes, central Mexico. J. Petrol. 46, 1243–1282.
Schmidt, M.W., Vielzeuf, D., Auzanneau, E., 2004. Melting and dissolution of subducting crust at high pressures: the key role of white mica. Earth Planet. Sci. Lett. 228, 65–84.
Sen, C., Dunn, T., 1994. Dehydration melting of a basaltic composition amphibolite at 1.5 and 2.0 GPa — implications for the origin of adakites. Contrib. Mineral. Petrol. 117, 394–409.
Siebe, C., Rodriguez-Lara, V., Schaaf, P., Abrams, M., 2004. Geochemistry, Sr–Nd isotope composition, and tectonic setting of Holocene Pelado, Guespalapa and Chichinautzin scoria cones, south of Mexico city. J. Volcanol. Geotherm. Res. 130, 197–226.
Skora, S., Blundy, J., 2010. High-pressure hydrous phase relations of radiolarian clay and implications for the involvement of subducted sediment in arc magmatism. J. Petrol. 51, 2211–2243.
Soper, D.S., 2013. p-Value Calculator for Correlation Coefficients [Software]. Available from http://www.danielsoper.com/statcalc.
Stern, C.R., Kilian, R., 1996. Role of the subducted slab, mantle wedge and continental crust in the generation of adakites from the Andean Austral volcanic zone. Contrib. Mineral. Petrol. 123, 263–281.
Straub, S.M., LaGatta, A.B., Pozzo, A., Langmuir, C.H., 2008. Evidence from high-Ni olivines for a hybridized peridotite/pyroxenite source for orogenic andesites from the central Mexican Volcanic Belt. Geochem. Geophys. Geosyst. 9.
Straub, S.M., Gómez-Tuena, A., Stuart, F.M., Zellmer, G.F., Espinasa-Perena, R., Cai, Y., Iizuka, Y., 2011. Formation of hybrid arc andesites beneath thick continental crust. Earth Planet. Sci. Lett. 303, 337–347.
Sun, S.S., McDonough, W.F., 1989. Chemical and isotopic systematics of oceanic basalts: implications for mantle composition and processes, Magmatism in the ocean basins, Geological Society Special Publication. pp. 313–345.
Suter, M., Martínez, M.L., Legorreta, O.Q., Martínez, M.C., 2001. Quaternary intra-arc extension in the central Trans-Mexican volcanic belt. Geol. Soc. Am. Bull. 113, 693–703.
Syracuse, E.M., van Keken, P.E., Abers, G.A., 2010. The global range of subduction zone thermal models. Phys. Earth Planet. Inter. 183, 73–90.
Tanaka, T., Togashi, S., Kamioka, H., Amakawa, H., Kagami, H., Hamamoto, T., Yuhara, M., Orihashi, Y., Yoneda, S., Shimizu, H., Kunimaru, T., Takahashi, K., Yanagi, T., Nakano, T., Fujimaki, H., Shinjo, R., Asahara, Y., Tanimizu, M., Dragusanu, C., 2000. JNdi-1: a neodymium isotopic reference in consistency with LaJolla neodymium. Chem. Geol. 168, 279–281.
Tatsumi, Y., Hanyu, T., 2003. Geochemical modeling of dehydration and partial melting of subducting lithosphere: toward a comprehensive understanding of high-Mg andesite formation in the Setouchi volcanic belt, SW Japan. Geochem. Geophys. Geosyst. 4.
Thorkelson, D.J., Breitsprecher, K., 2005. Partial melting of slab window margins: genesis of adakitic and non-adakitic magmas. Lithos 79, 25–41.
Tiepolo, M., Oberti, R., Zanetti, A., Vannucci, R., Foley, S.F., 2007. Trace-element partitioning between amphibole and silicate melt. Amphiboles Cryst. Chem. Occurrence Health Issues 67, 417–451.
Tollstrup, D., Gill, J., Kent, A., Prinkey, D., Williams, R., Tamura, Y., Ishizuka, O., 2010. Across-arc geochemical trends in the Izu–Bonin arc: contributions from the subducting slab, revisited. Geochem. Geophys. Geosyst. 11.
Torres-Alvarado, I.S., Smith, A.D., Castillo-Roman, J., 2011. Sr, Nd and Pb isotopic and geochemical constraints for the origin of magmas in Popocatepetl volcano (central Mexico) and their relationship with the adjacent volcanic fields. Int. Geol. Rev. 53, 84–115.
Urrutia-Fucugauchi, J., 1996. Bouguer gravity anomalies and regional crustal structure in Central Mexico. Int. Geol. Rev. 38, 176–194.
Van De Flierdt, T., Frank, M., Lee, D.C., Halliday, A.N., Reynolds, B.C., Hein, J.R., 2004. New constraints on the sources and behavior of neodymium and hafnium in seawater from Pacific Ocean ferromanganese crusts. Geochim. Cosmochim. Acta 68, 3827–3843.
van Westrenen, W., Blundy, J., Wood, B., 1999. Crystal–chemical controls on trace element partitioning between garnet and anhydrous silicate melt. Am. Mineral. 84, 838–847.
Verma, S.P., 2000. Geochemistry of the subducting Cocos plate and the origin of subduction-unrelated mafic volcanism at the volcanic front of the central Mexican Volcanic Belt. Geol. Soc. Am. Spec. Pap. 334, 195–222.
Vervoort, J.D., Blichert-Toft, J., 1999. Evolution of the depleted mantle: Hf isotope evidence from juvenile rocks through time. Geochim. Cosmochim. Acta 63, 533–556.
Vervoort, J.D., Patchett, P.J., Blichert-Toft, J., Albarède, F., 1999. Relationships between Lu–Hf and Sm–Nd isotopic systems in the global sedimentary system. Earth Planet. Sci. Lett. 168, 79–99.
Vervoort, J.D., Patchett, P.J., Albarède, F., Blichert-Toft, J., Rudnick, R., Downes, H., 2000. Hf–Nd isotopic evolution of the lower crust. Earth Planet. Sci. Lett. 181, 115–129.
Vervoort, J.D., Plank, T., Prytulak, J., 2011. The Hf–Nd isotopic composition of marine sediments. Geochim. Cosmochim. Acta 75, 5903–5926.
Wallace, P.J., Carmichael, I.S.E., 1999. Quaternary volcanism near the Valley of Mexico: implications for subduction zone magmatism and the effects of crustal thickness variations on primitive magma compositions. Contrib. Mineral. Petrol. 135, 291–314.
Watkins, J.S., McMillen, K.J., Bachman, S.B., Shipley, T.H., Moore, J.C., Angevine, C., 1981. Tectonic synthesis, leg 66: transect and vicinity. Initial Rep. Deep Sea Drill. Proj. 66, 837–849.
Weis, D., Kieffer, B., Hanano, D., Silva, I.N., Barling, J., Pretorius, W., Maerschalk, C., Mattielli, N., 2007. Hf isotope compositions of US Geological Survey reference materials. Geochem. Geophys. Geosyst. 8.
Whittaker, J.M., Miffler, R.D., Sdrolias, M., Heine, C., 2007. Sunda-Java trench kinematics, slab window formation and overriding plate deformation since the Cretaceous. Earth Planet. Sci. Lett. 255, 445–457.
Woodhead, J.D., Hergt, J.M., Davidson, J.P., Eggins, S.M., 2001. Hafnium isotope evidence for 'conservative' element mobility during subduction zone processes. Earth Planet. Sci. Lett. 192, 331–346.
Workman, R.K., Hart, S.R., 2005. Major and trace element composition of the depleted MORB mantle, DMM. Earth Planet. Sci. Lett. 231, 53–72.
Xiong, X.L., Keppler, H., Audetat, A., Ni, H.W., Sun, W.D., Li, Y.A., 2011. Partitioning of Nb and Ta between rutile and felsic melt and the fractionation of Nb/Ta during partial melting of hydrous metabasalt. Geochim. Cosmochim. Acta 75, 1673–1692.
Yang, T.F., Lee, T., Chen, C.-H., Cheng, S.-N., Knittel, U., Punongbayan, R.S., Rasdas, A.R., 1996. A double island arc between Taiwan and Luzon: consequence of ridge subduction. Tectonophysics 258, 85–101.
Yogodzinski, G.M., Kay, R.W., Volynets, O.N., Koloskov, A.V., Kay, S.M., 1995. Magnesian andesite in the Western Aleutian Komandorsky Region — implications for slab melting and processes in the mantle wedge. Geol. Soc. Am. Bull. 107, 505–519.
Yogodzinski, G.M., Lees, J.M., Churikova, T.G., Dorendorf, F., Woerner, G., Volynets, O.N., 2001. Geochemical evidence for the melting of subducting oceanic lithosphere at plate edges. Nature 409, 500–504.